

Hydrogen Adsorption Properties of Lantern-Type Dinuclear $M(BDC)(DABCO)_{1/2}$

Tohru Takei,[1] Jiro Kawashima,[1] Takato Ii,[1] Akihiro Maeda,[1] Mika Hasegawa,[1] Tamami Kitagawa,[1] Tetsushi Ohmura,[1] Masao Ichikawa,[2] Mitsuya Hosoe,[2] Izuru Kanoya,[2] and Wasuke Mori*[1]

[1]Department of Chemistry, Faculty of Science, Kanagawa University, Hiratsuka 259-1293

[2]Honda R & D Co., Ltd., Wako Research Center, Chuo, Wako 351-0193

Received October 11, 2007; E-mail: wmori@kanagawa-u.ac.jp

The hydrogen adsorption properties and uptake capacities of three-dimensional microporous materials of lantern-type dinuclear $M(BDC)(DABCO)_{1/2}$ ($M = Co^{II}$, Cu^{II}, and Zn^{II}; BDC = 1,4-benzenedicarboxylate, DABCO = 1,4-diazabicyclo[2.2.2]octane; $Co(BDC)(DABCO)_{1/2}$ (**1**), $Cu(BDC)(DABCO)_{1/2}$ (**2**), $Zn(BDC)(DABCO)_{1/2}$ (**3**)) were investigated at various temperatures of 77–333 K and pressures up to 10 MPa using a PCT automatic measuring system (Sievert-type apparatus). The results indicated that uptake to 4.11, 2.70, and 3.17 wt % of hydrogen can be stored on **1**, **2**, and **3**, respectively, at 77 K. The amounts of hydrogen are adsorbed by all complexes at around room temperature (293 K) and high-pressures are much lower (<0.5 wt %). Adsorption isotherms at around room temperature show a linear uptake relationship; all of them follow the Henry's law. By measuring nitrogen gas adsorption/desorption, all complexes exhibit approximately Type-I isotherms according to the IUPAC classification and possess BET surface areas in the range of 1165 (for **3**) to 1595 $m^2 g^{-1}$ (for **1**). Further, the thermal stability of all complexes is high, in the range of about 500 K (for **3**) to 600 K (for **1**). These complexes were synthesized and characterized by X-ray powder diffraction pattern, TG/DTA, FT-IR, surface area analysis, and hydrogen adsorption measurements.

The mineral zeolite was reported by Cronstedt in 1756 and Damour in 1840.[1] In the 20th century, numerous porous compounds (either natural or artificial) have become recognized. Zeolite, porous silica, clay, activated carbon, carbon fabric, etc. are well-known classical porous materials.[2] They are classified by their components (organic and inorganic), the degree of crystallization, pore size, and function.

Recently, a great deal of attention has been directed toward the use of coordination polymers in the design and synthesis of new porous materials.[3] Compared with conventional porous materials such as zeolites or activated carbons, these coordination polymers have future potential because they enable the design of desirable pore shapes and sizes, high microporosity, and flexible frameworks based on a variety of coordination geometries of metal centers and the multifunctionality of bridging organic ligands.[4] Such materials have been extensively studied in recent years because of their intriguing structures and, more importantly, for their potential applications in gas storage,[5] separation,[6] ion exchange,[7] and catalysis.[6e,8] These materials include a wide variety of coordination polymers having microporous structures, which usually accommodate guest molecules such as solvent molecules and/or counter ions.[9] The microporous structures are usually retained as far as the guest molecules are accommodated. Reversible removal and re-adsorption of guest molecules in solids without collapse of cavities or channel structures is a much less common phenomenon in solids of coordination polymers. Therefore, construction of robust compounds includes the properties that a channel or a cavity allows reversible adsorption and desorption of guest molecules without collapse of the microporous structure. For the porous properties, it is significant to build a well-associated network from a metal–organic ligand system.

The technology already exists in the form of fuel cells to convert stored chemical energy, in the form of hydrogen gas, directly into electrical energy with high efficiency.[10] The crucial factor that is hindering progress towards commercial implementation of these devices is the safe and efficient storage of the hydrogen fuel. Conventional storage of large amounts of hydrogen in its molecular form is difficult and expensive because it requires employing either extremely high-pressure to maintain it as a gas or very low temperature to maintain it as a liquid.[11] The development of storage media designed to overcome this difficulty is at the forefront of current research. The U.S. Department of Energy, in its Year 2010 Guidelines, has set performance targets for on-board automobile storage systems to have densities of 60 mg H_2/g (gravimetric) and 45 g H_2/L (volumetric).[12] Given that these are system goals, a practical material will need to have higher capacity when the weight of the tank and associated cooling or regeneration equipment is considered. The size and weight of these components will vary substantially depending on whether the material is operated by a chemisorption or physisorption mechanism. Hydrogen storage materials fall into two categories: those that dissociate the molecules and chemically bind them as hydrides and those that physisorb the molecules on their surface. Clearly, the most important attributes of the second class are high surface area and strong binding potential. Of the various materials under consideration, ordered porous materials such as metal–organic frameworks (MOFs) are considered capable of fulfilling this role. Recent studies have confirmed that these

Published on the web July 10, 2008; doi:10.1246/bcsj.81.847

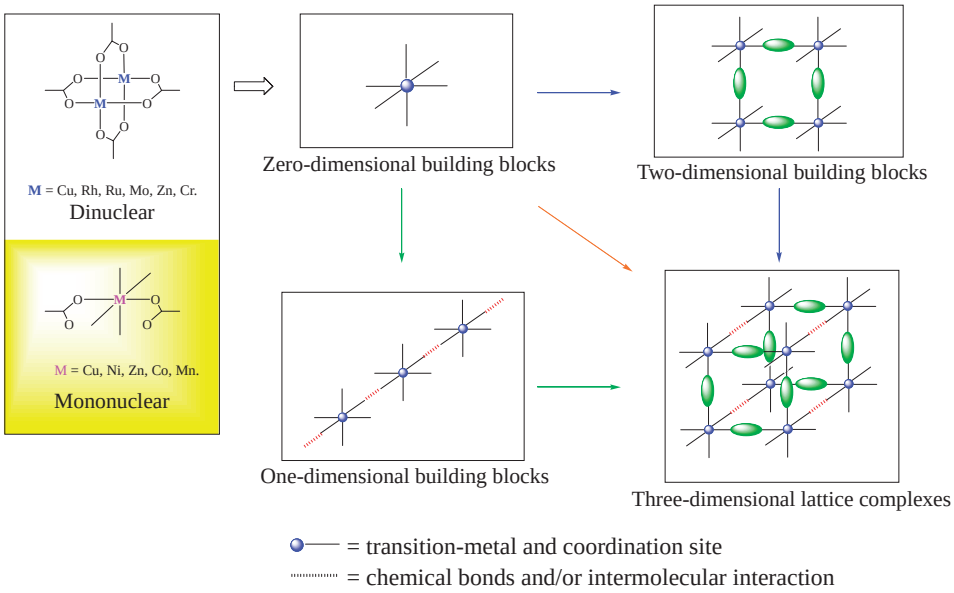

Figure 1. 3-D lattice organized by the assembly of lower dimensional building blocks.

frameworks can store considerable quantities of hydrogen at 77 K.[13]

Previously, we discovered that copper(II) terephthalate[3a,5a] occluded a large amount of nitrogen gas; various transition-metal dicarboxylates were synthesized as the first step in producing new porous materials. Polydentate ligands are suitable for producing stable covalent networks (softness of the structure is required). The use of molecular assemblies is also favorable for producing porous complexes in the solid state. The general method for synthesizing a three-dimensional (3-D) porous complex is shown in Figure 1. The intermolecular interactions are more important for producing porous structures consisting of lower dimensional building blocks. The ideal pores of complexes should have no disturbing molecules such as counter ions, so it is recommended that the complex skeleton be neutral. However, the counter ions of the pores sometimes play an important role in ion-exchange reactions. Further, we reported that copper(II) dicarboxylates,[14] molybdenum(II) dicarboxylates,[15] and ruthenium(II,III) dicarboxylates[16] reversibly occluded large amounts of gases such as N_2, Ar, O_2, CH_4, and Xe. The uniform linear micropores of these adsorbents were determined as having been constructed by the stacking or bonding of two-dimensional (2-D) lattices of dinuclear transition-metal dicarboxylates. Furthermore, it has been found that mononuclear copper(II) BDC–pyridine,[17] which has a regular one-dimensional (1-D) structure, occludes large amounts of gases.

In this paper, we report the synthesis and characterization of a series of lantern-type coordination polymers with 3-D network structures by linking original 2-D layer frameworks for mononuclear metal(II) BDC–pyridine with a pillar ligand such as DABCO. These 3-D polymers are expected to have larger porosities and higher stabilities than those of the original 2-D polymers. We present the hydrogen storage characteristics of three different samples of 3-D microporous materials of lantern-type dinuclear $M(BDC)(DABCO)_{1/2}$ under 77–333 K and different pressures, and correlate the maximum hydrogen storage capacity with their specific surface area.

Experimental

Materials and Characterization of Compounds. Cobalt(II) acetate tetrahydrate, copper(II) formate tetrahydrate, zinc(II) acetate dihydrate, terephthalic acid, methanol (99.8%), and pyridine (99.5%) were purchased from Wako Pure Chemical Industries Ltd. 1,4-Diazabicyclo[2.2.2]octane (DABCO) was purchased from Tokyo Chemical Industry Co., Ltd. Carbon, hydrogen, and nitrogen analysis were conducted using a Perkin-Elmer PE 2400 series-II CHNS/O analyzer. Fourier transform infrared (FT-IR) spectra were measured with a Jasco Co., FT/IR-300 spectrophotometer in the region of 4000–400 cm^{-1} using KBr discs. Absorption peaks were assigned as follows: very strong (vs), strong (s), medium (m), and weak (w). X-ray powder diffraction analysis data were recorded on a Bruker MF18XH22 diffractometer operated at 18 kW (400 mA) power for Cu Kα ($\lambda = 1.54056$ Å) with a scan speed of 4° min^{-1} and a step size of 0.020° in 2θ. Thermogravimetric/differential thermal analysis was conducted using TG8101D and TAS300 with an aluminum pan in an ordinary atmosphere. Samples were heated between room temperature and 773 K at 1–4 K min^{-1}.

N_2 Adsorption Measurement. Nitrogen adsorption/desorption isotherms were measured using an ASAP2010 volumetric adsorption apparatus provided by Micromeritics Co., Ltd. Before adsorption measurements, the samples were degassed under vacuum at 373 K. Nitrogen adsorption/desorption isotherms were measured in the relative pressure (P/P_0, P_0 = saturation pressure) range of 10^{-6} to 1. The linear region of the nitrogen isotherm used for the BET surface area plot was $0.02 < P/P_0 < 0.10$, and for the Langmuir surface area plot the range was $0.02 < P/P_0 < 0.35$. The apparent surface areas were calculated using a molecular cross-sectional area of 0.162 nm^2 for both models. The pore volume was determined by extrapolating the Dubinin–Radushkevich (DR) equation[18] across the linear region of the low-pressure data points with the assumption that the density of the adsorbate in the pore was the same as that of the pure adsorbate in its liquid state.

Ar Adsorption Measurement. Argon adsorption isotherms were measured using an ASAP2010 volumetric adsorption

apparatus provided by Micromeritics Co., Ltd. Before the adsorption measurements, the samples were degassed under a vacuum at 373 K. Argon adsorption isotherms were measured in the relative pressure (p/p_0, p_0 = saturation pressure) range of 10^{-6} to 1.

H_2 High-Pressure Adsorption Measurement. Hydrogen adsorption and desorption capacities were determined at 77–333 K by PCT automatic measuring systems (Sievert-type apparatus, maximum pressure: 10 MPa) provided by Suzuki Shokan Co., Ltd., Japan. The hydrogen adsorption and desorption capacities were calculated from densities of about 1.700, 1.659, and 1.612 g cm^{-3} for compounds **1**, **2**, and **3**, respectively. The grade of hydrogen used in this work was >99.99999%. The mass of the compounds used for hydrogen storage measurements was 0.2–0.3 g. Prior to measurement, the samples were degassed and heated at 373 K for approximately 2 h at a pressure of 0.1 MPa.

Co(BDC)(DABCO)$_{1/2}$. An aqueous solution (100 mL) of cobalt(II) acetate tetrahydrate (0.25 g) was added to a pyridine solution (400 mL) of terephthalic acid (0.2 g). After mixing, the solution was allowed to stand for several days at room temperature forming a pink, plate-like crystal precipitate.[19] A methanol solution (100 mL) of DABCO (0.1 g) was added to the pink, plate-like crystal precipitate (0.1 g) and the mixture was stirred for about 24 h at 338 K. A purplish-red powder capable of adsorbing gases was collected, washed with methanol, and dried at 373 K under vacuum for 4 h (yield: 67.7%) (complex **1**). [$Co^{II}(O_2CC_6H_4CO_2)$-$(N_2C_6H_{12})_{0.5}$] (**1**): Anal. Calcd for $C_{11}H_{10}CoN_1O_4$: C, 47.33; H, 3.61; N, 5.02%. Found: C, 47.27; H, 3.58; N, 4.91%. FT-IR (KBr disk, 4000–400 cm^{-1}) 1575vs, 1502m, 1467w, 1381vs, 1316m, 1149w, 1104w, 1053w, 1014w, 805m, 748m, 697m, 610m, 518m, 451m cm^{-1}.

Cu(BDC)(DABCO)$_{1/2}$. An aqueous solution (100 mL) of copper(II) formate tetrahydrate (0.5 g) was added to a pyridine solution (100 mL) of terephthalic acid (0.37 g). After mixing, the solution was allowed to stand for several days at room temperature forming a blue, plate-like crystal precipitate.[17] A methanol solution (100 mL) of DABCO (0.027 g) was added to the blue, plate-like crystal precipitate (0.1 g) and the mixture was stirred for about 2 days at room temperature. A greenish-blue powder capable of adsorbing gases was collected, washed with methanol, and dried at 373 K under vacuum for 2 h (yield: 73.8%) (complex **2**). [$Cu^{II}(O_2CC_6H_4CO_2)(N_2C_6H_{12})_{0.5}$] (**2**): Anal. Calcd for $C_{11}H_{10}CuN_1O_4$: C, 46.56; H, 3.55; N, 4.94%. Found: C, 46.53; H, 3.47; N, 5.14%. FT-IR (KBr disk, 4000–400 cm^{-1}) 1587s, 1504m, 1388vs, 1150w, 1093w, 1053m, 1013w, 889w, 829m, 748m, 669m, 569m, 501w, 464w, 417w cm^{-1}.

Zn(BDC)(DABCO)$_{1/2}$. An aqueous solution (100 mL) of zinc(II) acetate dihydrate (0.5 g) was added to a pyridine solution (400 mL) of terephthalic acid (0.38 g). After mixing, the solution was allowed to stand for several days at room temperature forming a colorless, plate-like crystal precipitate.[17] A methanol solution (100 mL) of DABCO (0.2 g) and benzene (10 mL) was added to the colorless, plate-like crystal precipitate (0.1 g) and the mixture was stirred for about 2 days at room temperature. A colorless powder capable of adsorbing gases was collected, washed with methanol, and dried at 373 K under vacuum for 2 h (yield: 90.4%) (complex **3**). [$Zn^{II}(O_2CC_6H_4CO_2)(N_2C_6H_{12})_{0.5}$] (**3**): Anal. Calcd for $C_{11}H_{10}ZnN_1O_4$: C, 46.26; H, 3.53; N, 4.90%. Found: C, 46.21; H, 3.30; N, 4.97%. FT-IR (KBr disk, 4000–400 cm^{-1}) 1570vs, 1503m, 1381vs, 1160w, 1112w, 1053m, 1011w, 886w, 830m, 745s, 658w, 557w, 514w, 446w cm^{-1}.

Results and Discussion

Structural Characterization. The so-called "pillaring" strategy in designing metal–organic frameworks involves using appropriate pillars to connect well-defined 2-D layers either in a one-pot reaction[20] or in two separate steps.[21] Throughout a series of preliminary experiments,[17] we noticed that diffusional reactions of transition metals, aromatic dicarboxylic acids, and pyridine rings predominantly produce 2-D layered structures with 1-D micropores. Lantern-type 3-D coordination polymers of M(BDC)(DABCO)$_{1/2}$ were synthesized by heterogeneous reactions between mononuclear metal(II) BDC–pyridine and DABCO as a pillar ligand. It succeeded in syntheses of lantern-type cobalt(II) dicarboxylates,[19] which was not reported to form lantern-type dinuclear structure by using a mononuclear complex as starting materials. Furthermore, the reactions are reproducible and can be readily scaled up to produce gram quantities.

The structures and stabilities of 3-D coordination polymers were studied by X-ray powder diffraction (XRPD) patterns and thermal gravimetric (TG) analysis. Figure 2 shows that the observed XRPD patterns are in good accordance with the simulated patterns of the optimized Cu(BDC)(DABCO)$_{1/2}$[5f] structure by using Cerius2, confirming that the structures of the obtained compounds are plausible. Based on these results and elemental analyses, this structure is supposed to be lantern-type 3-D. The 2-D layers bridging the metal(II) ions with the dicarboxylates ions are linked with DABCO as a pillar ligand, as shown in Figure 3.

Structural stability is an important factor in the study of the microporous functions of coordination polymers. Figure 4 suggests that the porous nets in this study have a thermal stability about 570 K under air. The results showed that M(BDC)(DABCO)$_{1/2}$ has high thermal stability with no chemical decomposition between room temperature and 500–600 K, in comparison with the starting material, M(BDC)(Py). For all the complexes, the XRPD patterns were measured at different temperatures to unambiguously establish the stability of its bulk phase. The fully evacuated open structures were found to be stable up to at least 573 K under an inert gas (Figure 5).

N_2/Ar Adsorption Properties. Specific surface area is one of the most important factors for evaluating pore capacity, and is associated with the number of guest molecules accommodated by direct contact. The porosity and specific surface areas of metal–organic porous materials **1**–**3** were estimated by measuring nitrogen gas adsorption/desorption isotherms at 77 K in a relative pressure range of 10^{-6} to 1. Strictly speaking, the mechanism of adsorption in microporous material (pores < 2 nm) is pore filling as opposed to mono/multilayer adsorption. Therefore, applications of the Langmuir or BET methods only give rise to apparent surface areas and are reported in order to facilitate comparisons with other materials. Analyses of these isotherms yielded Langmuir surface areas, BET surface areas, maximum micropore volumes (using DR methods and Horvath–Kawazoe (HK) methods[22]) for all complexes shown in Table 1. The nitrogen gas adsorption/desorption isotherms are shown in Figure 6a. Isotherm plots for nitrogen adsorption/desorption of all complexes against relative pressure do not show the significant hysteresis. In all cases,

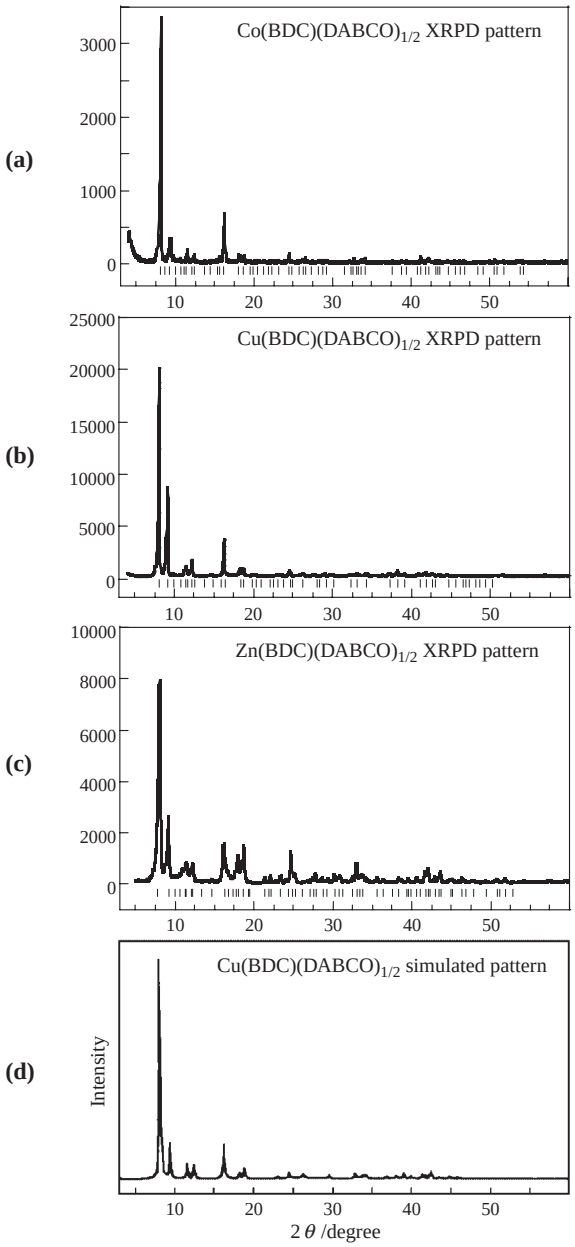

Figure 2. XRPD patterns for all complexes. (a) Co(BDC)-(DABCO)$_{1/2}$. (b) Cu(BDC)(DABCO)$_{1/2}$. (c) Zn(BDC)-(DABCO)$_{1/2}$. (d) Simulated XRPD pattern for Cu(BDC)-(DABCO)$_{1/2}$.[5f]

the adsorption of nitrogen reaches near-saturation at low relative pressures ($P/P_0 < 0.05$) and thereafter increases very slowly up to 1 atm. The adsorption isotherms of nitrogen for all complexes can be interpreted as Type-1 of the Langmuir type adsorption isotherm, implying that the cavities in all these materials consist of micropores but there are no large cavities, which may be classified as mesopores. The sharp rise of nitrogen adsorption at low relative pressures indicates that the micropores are uniform. The rise of nitrogen adsorption at high relative pressures depends on condensation into interparticle voids. With an approximation based on a monolayer condensation of adsorbed nitrogen molecules on a uniform surface, the sorption isotherms were fitted to a Langmuir equation and

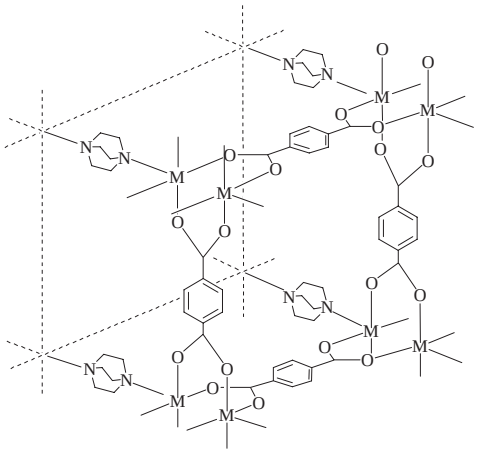

Figure 3. Plausible lantern-type 3-D structure for M(BDC)(DABCO)$_{1/2}$ [M = Co^{II}, Cu^{II}, and Zn^{II}].

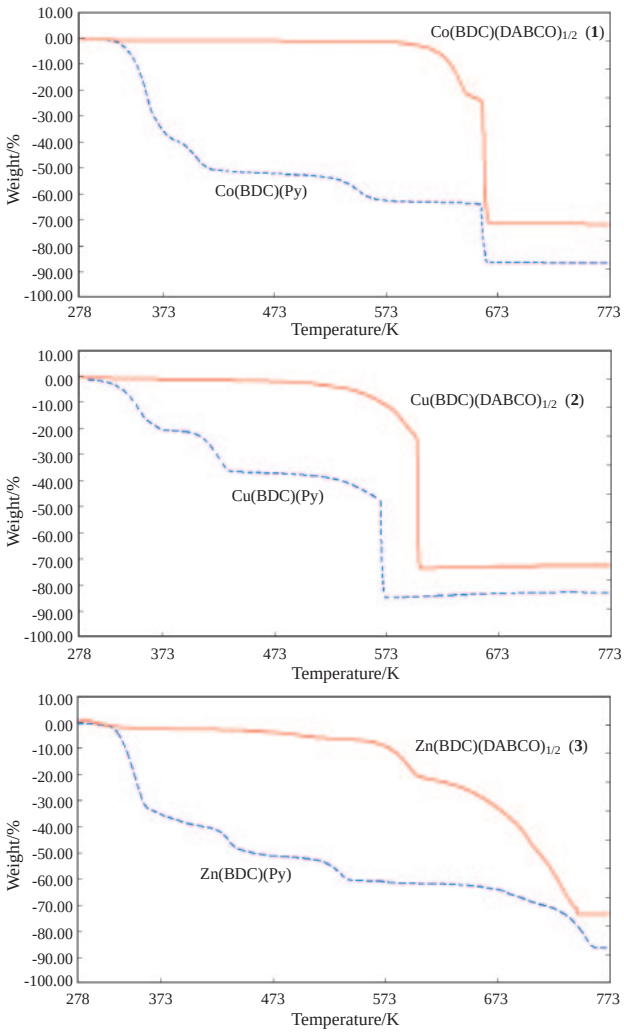

Figure 4. TG curves of M(BDC)(DABCO)$_{1/2}$ and M(BDC)(Py) [starting materials]. M(BDC)(DABCO)$_{1/2}$ data is shown as a solid line, M(BDC)(Py) data as a dashed line. Top: Co(BDC)(DABCO)$_{1/2}$; Middle: Cu(BDC)-(DABCO)$_{1/2}$; Bottom: Zn(BDC)(DABCO)$_{1/2}$.

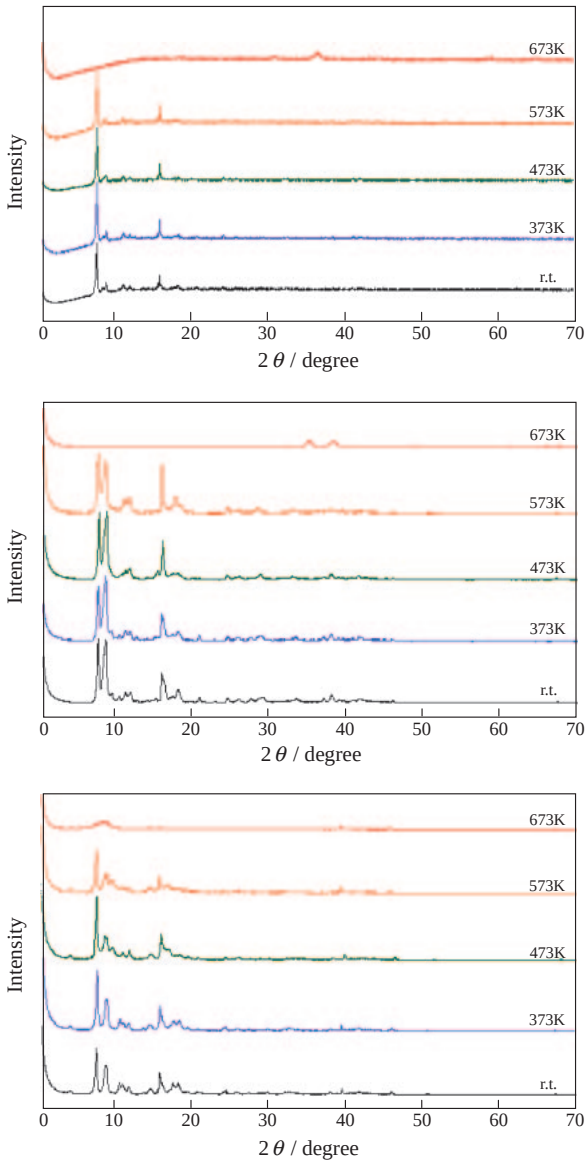

Figure 5. Temperature progression of XRPD pattern for all complexes measured in inert gas. The sample was held at designated temperatures for at least 10 min. Top: $Co(BDC)(DABCO)_{1/2}$; Middle: $Cu(BDC)(DABCO)_{1/2}$; Bottom: $Zn(BDC)(DABCO)_{1/2}$.

gave surface areas for the frameworks from 1488 (for **3**) to 2120 $m^2 g^{-1}$ (for **1**). The maximum pore volume, which is the volume adsorbed at STP when P/P_0 approaches 1, ranges from 0.63 (for **3**) to 0.77 $cm^3 g^{-1}$ (for **1**). However, compared with the actual surface areas, the isotherm values are generally small because of irregularities in the walls of the adsorbent. The BET surface areas are generally 25–30% less than the Langmuir surface areas, as is often recorded in the articles. The difference between the values of the surface area obtained with the BET and the Langmuir models results from the fact that neither model adequately describes the nitrogen adsorption isotherms of microporous materials.

The effective pore size distributions by measuring argon gas (using HK methods) are shown in Figure 6b. In each sample, a single sharp peak is observed ca. 6.0 Å, indicating that the complexes have uniform micropores. The effective pore sizes were 6.13, 5.96, and 6.18 Å for materials **1**, **2**, and **3**, respectively.

Low-Pressure Hydrogen Adsorption. In general, the behavior of adsorption in a pore is different according to the diameter of the pore. It is a known fact that the energy of the interaction of hydrogen with adsorbent surfaces is low.[23] However, the interaction potential can be enhanced in pores with sizes close to that of the hydrogen molecule (ca. 0.3 nm)[24] because of the overlap of the potential fields from the pore walls. Therefore, pores that are slightly larger than a molecule's diameter are important for a high degree of hydrogen adsorption.

As expected from their large porosities, the materials adsorb considerable amounts of hydrogen. Figure 7 shows the resulting hydrogen adsorption/desorption isotherms up to 0.1 MPa at 77 K. Under these conditions, hydrogen adsorption isotherms are not saturated because these temperatures are above the critical temperature (33 K for hydrogen). The hydrogen adsorption properties of all complexes are listed in Table 2. For materials of this class, the hydrogen adsorption isotherms are Type-1, as expected for microporous materials. Low-pressure, high-resolution hydrogen adsorption measurements can provide useful information on gas–solid interactions between adsorbate and adsorbent. A characteristic feature that is clearly apparent from the hydrogen adsorption isotherm, shown in Figure 7, is the different slopes of the curves in the low-pressure range. All complexes in this study showed a faster rise in hydrogen uptake than in Yaghi's IRMOF-1.[13c] In general, the lower pressure range ($P/P_0 < 0.3$) in the BET isotherms is considered as the region where gas molecules cover the surface almost exclusively as a monolayer. Therefore, it might

Table 1. Summary of Porosity Measurements[a)]

Materials		$N2_{BET}$ /$m^2 g^{-1}$	$N2_{Lang}$ /$m^2 g^{-1}$	$N2_{vol}$ /$cm^3 g^{-1}$	$N2_{dia}$ /Å	Ar_{dia} /Å	N_2 per f.u.[b)]
$Co(BDC)(DABCO)_{1/2}$	(**1**)	1595	2120	0.77	4.7	6.13	12.5
$Cu(BDC)(DABCO)_{1/2}$	(**2**)	1300	1703	0.63	9.7	5.96	10.4
$Zn(BDC)(DABCO)_{1/2}$	(**3**)	1165	1488	0.63	5.3	6.18	10.4
IRMOF-1[5c,13b]		2900	3362	1.04	—	—	—
Kim's $Zn(BDC)(DABCO)_{1/2}$[13d]		1450	2090	0.75	—	—	12.3

a) Acronyms: $N2_{BET}$ and $N2_{Lang}$ are the BET and Langmuir surface areas by measuring nitrogen gas; $N2_{vol}$ is pore volume by measuring nitrogen gas; $N2_{dia}$ is pore diameter by measuring nitrogen gas; and Ar_{dia} is pore diameter by measuring argon gas. b) Formula units (f.u.) defined $[M_2(BDC)_2(DABCO)]$.

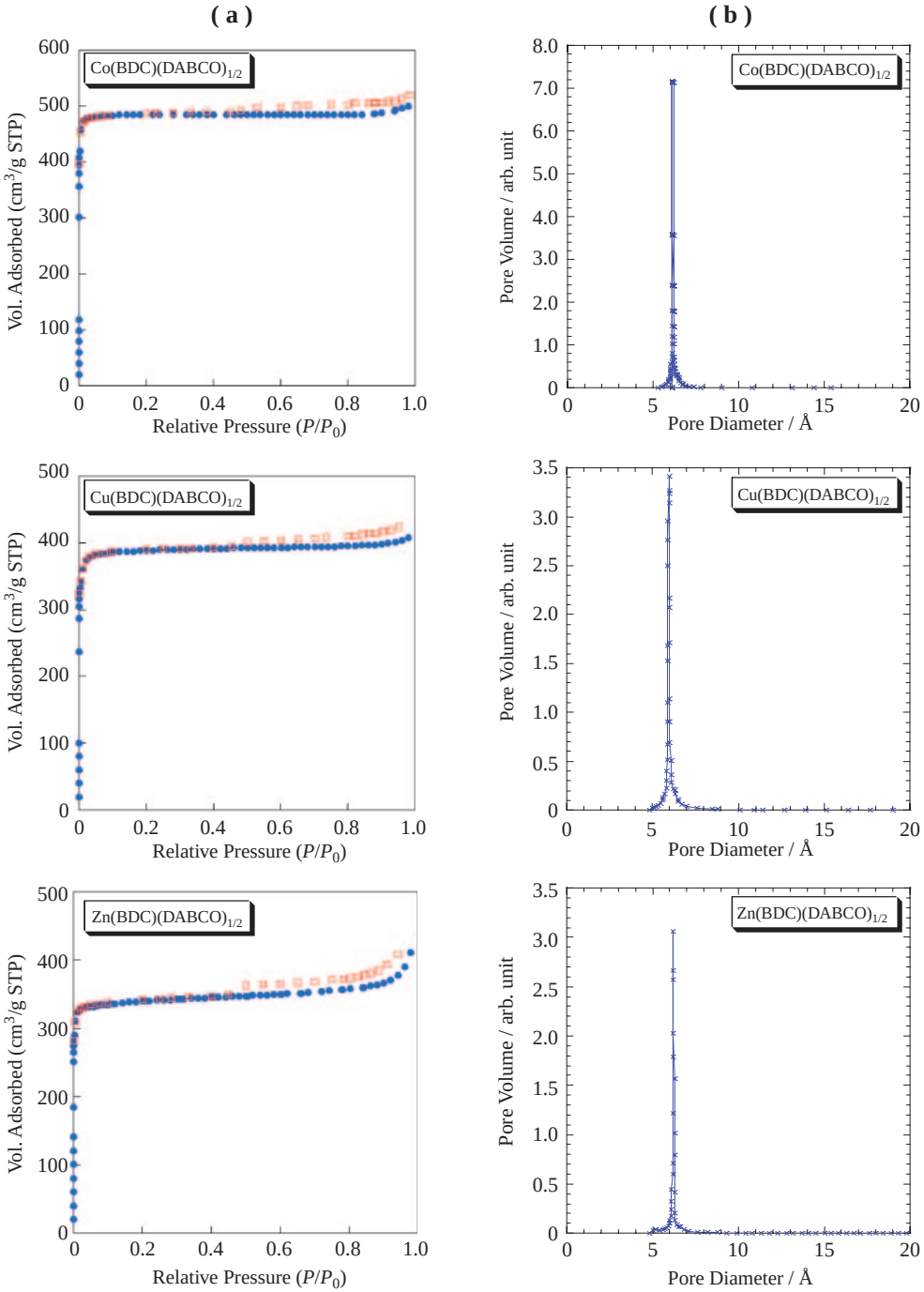

Figure 6. (a) Nitrogen adsorption/desorption isotherms at 77 K for all complexes. Adsorption data is indicated by filled circles, desorption data by open squares. Top: $Co(BDC)(DABCO)_{1/2}$; Middle: $Cu(BDC)(DABCO)_{1/2}$; Bottom: $Zn(BDC)(DABCO)_{1/2}$. (b) Pore size distribution by measuring argon gas for all complexes. Top: $Co(BDC)(DABCO)_{1/2}$; Middle: $Cu(BDC)(DABCO)_{1/2}$; Bottom: $Zn(BDC)(DABCO)_{1/2}$.

be that the affinity of hydrogen molecules toward the frameworks in this study is higher than in IRMOF-1. The maximum amounts of storage hydrogen gas ranged from 1.54 wt % for **3** to 2.28 wt % for **1**. These values are higher than are those of IRMOF-1[5c] under the same conditions. The results showed that no correlation existed between storage capacity and specific surface area. This result might be attributed to the difference in pore size, since complex **1–3** (ca. 6.0 Å) possesses a smaller size than does IRMOF-1 (ca. 8.0 Å;[5c,25] This value is measured by X-ray crystallography).

High-Pressure Hydrogen Adsorption. High-pressure hydrogen adsorption measurements were performed on a Sievert-type apparatus using a static volumetric technique. Figure 8a shows the resulting hydrogen adsorption/desorption isotherms up to 10 MPa at 77 K. As expected, all complexes adsorbed large amounts of hydrogen at low temperature. The isotherms show a Type-1 profile with an initial steep increase in hydrogen uptake followed by a plateau at high pressures. There is a

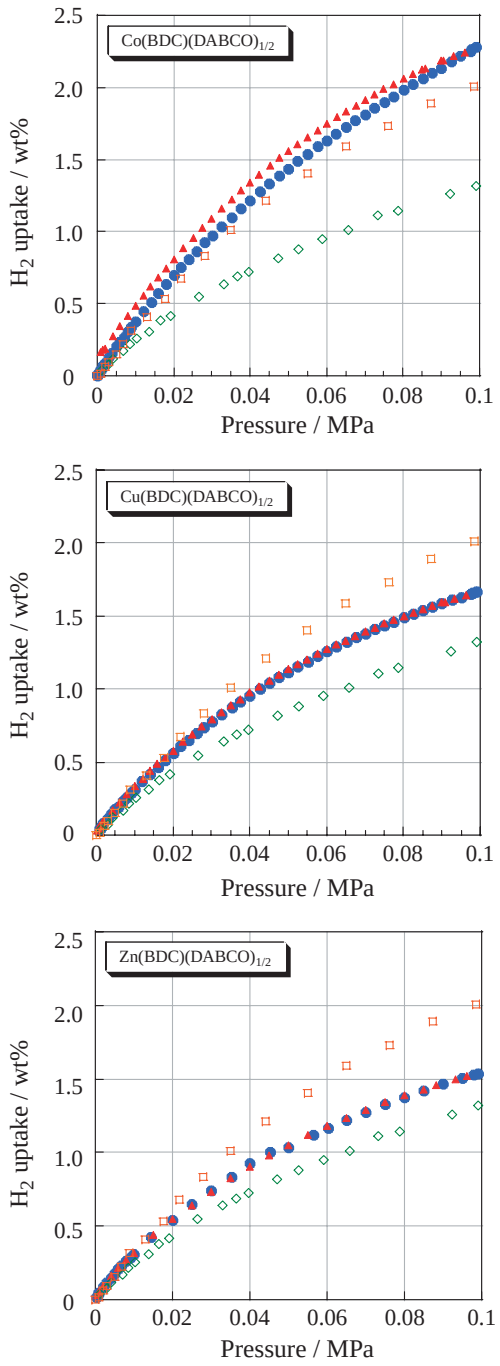

Figure 7. Hydrogen adsorption/desorption isotherms for $M(BDC)(DABCO)_{1/2}$ measured at 77 K and 0.1 MPa. Adsorption data is indicated by filled circles, desorption data by filled triangles, IRMOF-1 adsorption data[13b] by open diamonds, and Kim's $Zn(BDC)(DABCO)_{1/2}$ adsorption data[13f] by open squares. Top: $Co(BDC)(DABCO)_{1/2}$; Middle: $Cu(BDC)(DABCO)_{1/2}$; Bottom: $Zn(BDC)(DABCO)_{1/2}$.

hysteresis loop between adsorption and desorption under 1 MPa for **1**. All complexes reached saturation under 10 MPa at 77 K. The saturation uptakes vary widely: for **1**, the uptake at saturation is 4.11 wt % (4.42 MPa), for **2**, the uptake at saturation is 2.70 wt % (3.37 MPa), and for **3**, the uptake at saturation is 3.17 wt % (8.32 MPa). Complex **1** showed superior hydrogen adsorption at 77 K and 0.1 MPa compared with IRMOF-1. However, the quantity of maximum hydrogen adsorption reversed under high-pressure (77 K and 10 MPa) because the mechanism of adsorption in microporous material is pore filling in contrast to mono/multilayer adsorption. This result reveals that the best MOFs for hydrogen storage based on physisorption should possess a high pore volume.

Figure 8b shows the resulting hydrogen adsorption isotherms up to 10 MPa at 253, 273, 293, 313, and 333 K. The hydrogen adsorption properties of all complexes are listed in Table 2. At around room temperature, all complexes can only adsorb very small amounts of hydrogen and exhibit a linear uptake relationship (known as Henry's law[26]). Henry's law is predicted to be observed in the region of very low coverage, where interaction between adsorbed molecules can be neglected and the only remaining interactions are those between single molecules and the surface.[27] Such types of isotherms are typical for physical adsorption in microporous materials. The fall of the quantity of hydrogen caused by the temperature increase from 293 to 333 K of **1** and **2** were below 0.1 wt %. For comparison, IRMOF-1 ($Zn_4O(BDC)_3$) was reported to have a high-pressure hydrogen uptake <0.3 wt % of less than 6.5 MPa at 77 K.[13e]

Figure 9 shows that the maximum hydrogen uptake of each MOF, corresponding to the plateau of the adsorption isotherm of 77 K, correlates almost linearly with the specific surface area. Here, the specific surface area determined with the BET model is considered. This is conventionally reported in the literature even though not perfectly appropriate for microporous materials. Nevertheless, these BET values can be considered for qualitative comparisons. This correlation is independent of the framework structure and the central metal ions, which are indicated in the figure.

Conclusion

We have reported on high-pressure hydrogen storage at various temperatures in three porous metal–organic frameworks of lantern-type dinuclear $M(BDC)(DABCO)_{1/2}$. All complexes were synthesized using a new procedure, the reactions of which are reproducible and can be readily scaled up. These complexes exhibit extremely high thermal stability under vacuum.

Hydrogen adsorption/desorption measurements at 0.1 MPa and up to 10 MPa, confirm high hydrogen adsorption in these materials with excellent reversibility. At 77 K and high-pressure, $Co(BDC)(DABCO)_{1/2}$ has the highest storage capacity (4.11 wt %, 4.42 MPa) of all complexes. At 77 K and low-pressure, all complexes are promising hydrogen storage materials because of the steep rise in the adsorption isotherms. In particular, the quantity of hydrogen adsorption of $Co(BDC)(DABCO)_{1/2}$ was higher than that of IRMOF-1, Kim's $Zn(BDC)(DABCO)_{1/2}$, zeolites,[2f] and activated carbons[2g] under the same conditions. These results showed that high surface area and more suitable pore size are important under low-pressure. In addition, a higher porosity is important under high-pressure. Therefore, the major challenge is to synthesize MOFs having both an optimum pore size and high pore volume without decreasing the specific surface area. In contrast,

Table 2. Summary of Hydrogen Gas Adsorption Data[a)]

Materials		$N2_{BET}$ /m^2 g^{-1}	$HL_{77\,K}$ /wt %	$HH_{77\,K}$ /wt %	$HH_{253\,K}$ /wt %[b)]	$HH_{273\,K}$ /wt %[b)]	$HH_{293\,K}$ /wt %[b)]	$HH_{313\,K}$ /wt %[b)]	$HH_{333\,K}$ /wt %[b)]	H_2 per f.u.[c)]
$Co(BDC)(DABCO)_{1/2}$	(**1**)	1595	2.28	4.11 (4.42 MPa)	0.56	0.48	0.32	0.31	0.25	6.4
$Cu(BDC)(DABCO)_{1/2}$	(**2**)	1300	1.67	2.70 (3.37 MPa)	0.63	0.59	0.42	0.28	0.33	4.8
$Zn(BDC)(DABCO)_{1/2}$	(**3**)	1165	1.54	3.17 (8.32 MPa)	0.63	0.56	0.43	0.35	0.29	4.4
IRMOF-1[13d,13e]		2900	1.32	5.21 (4.54 MPa)	—	—	0.28[d)]	—	—	5.0
Kim's $Zn(BDC)(DABCO)_{1/2}$[13f]		1450	2.01	—	—	—	—	—	—	5.7
Zeolite (ZSM-5)[2f]		445	1.97	—	—	—	0.38	—	—	—
Activated carbon[2g]		2564	—	4.5 (6.5 MPa)	—	—	<0.5	—	—	—

a) Acronyms: $N2_{BET}$, is the BET surface areas by measuring nitrogen gas, $HL_{77\,K}$ is the maximum amounts of H_2 adsorbed at 0.1 MPa, 77 K; $HH_{77\,K}$ is the maximum amounts of H_2 adsorbed at 10 MPa, 77 K; $HH_{253\,K}$ is the maximum amounts of H_2 adsorbed at 10 MPa, 253 K; $HH_{273\,K}$ is the maximum amounts of H_2 adsorbed at 10 MPa, 273 K; $HH_{293\,K}$ is the maximum amounts of H_2 adsorbed at 10 MPa, 293 K; $HH_{313\,K}$ is the maximum amounts of H_2 adsorbed at 10 MPa, 313 K; $HH_{333\,K}$ is the maximum amounts of H_2 adsorbed at 10 MPa, 333 K. b) High-pressure hydrogen adsorption data from 253 to 333 K are converted into 10 MPa. c) Formula units (f.u.) defined $[M_2(BDC)_2(DABCO)]$. The condisions are at 0.1 MPa, 77 K. d) Maximum amount of H_2 adsorbed at 6.5 MPa, 298 K.

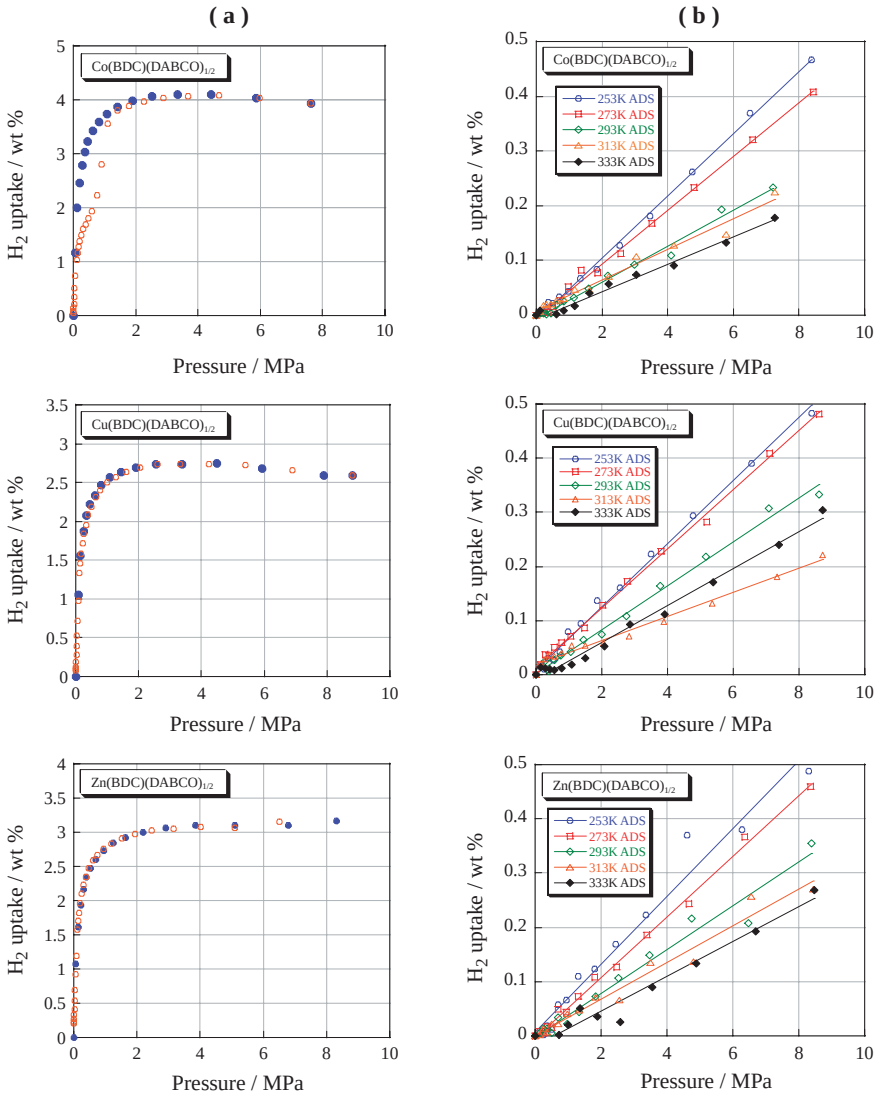

Figure 8. (a) Hydrogen adsorption/desorption isotherms for $M(BDC)(DABCO)_{1/2}$ measured at 77 K and 10 MPa. Adsorption data is indicated by filled circles, desorption data by open circles. Top: $Co(BDC)(DABCO)_{1/2}$; Middle: $Cu(BDC)(DABCO)_{1/2}$; Bottom: $Zn(BDC)(DABCO)_{1/2}$. (b) Hydrogen adsorption isotherms for $M(BDC)(DABCO)_{1/2}$ measured at various temperatures and 10 MPa. Top: $Co(BDC)(DABCO)_{1/2}$; Middle: $Cu(BDC)(DABCO)_{1/2}$; Bottom: $Zn(BDC)(DABCO)_{1/2}$.

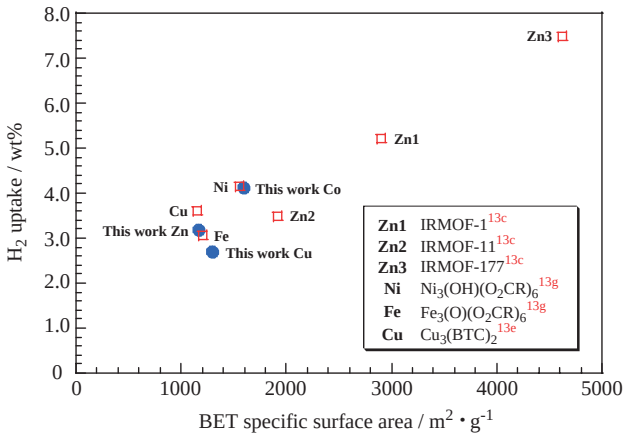

Figure 9. Maximum hydrogen uptake at 77 K of different MOFs versus their BET surface areas. The central metal ions of the MOFs are indicated.

at around room temperature (293 K) and at high-pressure, the hydrogen uptake is less than 0.5 wt %, which is reasonable considering the weak interaction involved in physisorption. It is not clear from the available results to date that increasing the pressure will be sufficient to increase the adsorption capacity at around room temperature to a level similar to that achieved at 77 K.

The results indicated that, at around room temperature, conventional porous metal–organic frameworks could not store the amount of hydrogen required for automotive applications. However, much of the periodic table has yet to be explored in pursuing open framework MOFs. We are currently exploring the synthesis of new inorganic clusters with new pore structure for high levels of hydrogen storage.

References

1 a) A. F. Cronstedt, *Akad. Hankle. Stockholm* **1756**, *18*, 120. b) A. Damour, *Ann. Mines* **1840**, *17*, 191.

2 a) R. K. Iler, *The Chemistry of Silica*, Wiley, New York, **1979**; R. Szostack, *Molecular Sieves*, 2nd ed., Blackie Academic and Professional, London, **1998**. b) L. L. Henchi, D. R. Ulrich, *Ultrastructure Processing of Ceramics, Glasses, and Composites*, Wiley, New York, **1984**. c) R. E. Grim, *Applied Clay Mineralogy*, McGraw-Hill, New York, **1962**. d) *Microporous and Macroporous Materials*, ed. by R. F. Lobo, J. S. Beck, S. L. Suib, D. R. Corbin, M. E. Davis, L. E. Iton, S. I. Zones, Materials Research Society, Pittsburgh, **1996**. e) M. G. Nijkamp, J. E. M. J. Raaymakers, A. J. van Dillen, K. P. de Jong, *Appl. Phys. A: Mater. Sci. Process.* **2001**, *72*, 619. f) X.-M. Du, E.-D. Wu, *Chin. J. Chem. Phys.* **2006**, *19*, 457. g) B. Panella, M. Hirscher, S. Roth, *Carbon* **2005**, *43*, 2209.

3 a) W. Mori, F. Inoue, K. Yoshida, H. Nakayama, S. Takamizawa, M. Kishita, *Chem. Lett.* **1997**, 1219. b) H. Li, M. Eddaoudi, T. L. Groy, O. M. Yaghi, *J. Am. Chem. Soc.* **1998**, *120*, 8571. c) S. Kitagawa, M. Kondo, *Bull. Chem. Soc. Jpn.* **1998**, *71*, 1739.

4 a) M. Munakata, L. P. Wu, T. Kuroda-Sowa, *Bull. Chem. Soc. Jpn.* **1997**, *70*, 1727. b) S. Decurtins, S. Ferlay, R. Pellaux, M. Gross, H. Schmalle, *Supramolecular Engineering of Synthetic Metallic Materials-Conductors and Magnets*, Kiuwer Academic Pub., **1999**.

5 a) W. Mori, T. Sato, C. N. Kato, T. Takei, T. Ohmura, *Chem. Rec.* **2005**, *5*, 336. b) T. Ohmura, A. Usuki, K. Fukumori, T. Ohta, M. Ito, K. Tatsumi, *Inorg. Chem.* **2006**, *45*, 7988. c) H. Li, M. Eddaoudi, M. O'Keeffe, O. M. Yaghi, *Nature* **1999**, *402*, 276. d) S. Kitagawa, R. Kitaura, S. Noro, *Angew. Chem., Int. Ed.* **2004**, *43*, 2334. e) S. Takamizawa, E. Nakata, T. Saito, T. Akatsuka, *Inorg. Chem.* **2005**, *44*, 1362. f) K. Seki, S. Takamizawa, W. Mori, *Chem. Lett.* **2001**, 332. g) B. D. Chandler, D. T. Cramb, G. K. H. Shimizu, *J. Am. Chem. Soc.* **2006**, *128*, 10403. h) G. Férey, C. Mellot-Draznieks, C. Serre, F. Millange, J. Dutour, S. Surblé, I. Margiolaki, *Science* **2005**, *309*, 2040. i) R.-Q. Zou, L. Jiang, H. Senoh, N. Takeichi, Q. Xu, *Chem. Commun.* **2005**, 3526.

6 a) J. Won, J. S. Seo, J. H. Kim, H. S. Kim, Y. S. Kang, S.-J. Kim, Y. Kim, J. Jegal, *Adv. Mater.* **2005**, *17*, 80. b) O. R. Evans, H. L. Ngo, W. Lin, *J. Am. Chem. Soc.* **2001**, *123*, 10395. c) R. Matsuda, R. Kitaura, S. Kitagawa, Y. Kubota, R. V. Belosludov, T. C. Kobayashi, H. Sakamoto, T. Chiba, M. Takata, Y. Kawazoe, Y. Mita, *Nature* **2005**, *436*, 238. d) L. Pan, D. H. Olson, L. R. Ciemnolonski, R. Heddy, J. Li, *Angew. Chem., Int. Ed.* **2006**, *45*, 616. e) J. S. Seo, D. Whang, H. Lee, S. I. Jun, J. Oh, Y. J. Jeon, K. Kim, *Nature* **2000**, *404*, 982.

7 a) B. F. Hoskins, R. Robson, *J. Am. Chem. Soc.* **1990**, *112*, 1546. b) O. M. Yaghi, H. Li, *J. Am. Chem. Soc.* **1995**, *117*, 10401. c) A. Kamiyama, T. Noguchi, T. Kajiwara, T. Ito, *Angew. Chem., Int. Ed.* **2000**, *39*, 3130. d) S. Noro, R. Kitaura, M. Kondo, S. Kitagawa, T. Ishii, H. Matsuzaka, M. Yamashita, *J. Am. Chem. Soc.* **2002**, *124*, 2568. e) E. Lee, J. Kim, J. Heo, D. Whang, K. Kim, *Angew. Chem., Int. Ed.* **2001**, *40*, 399.

8 a) W. Mori, S. Takamizawa, C. N. Kato, T. Ohmura, T. Sato, *Microporous Mesoporous Mater.* **2004**, *73*, 31. b) C. N. Kato, M. Hasegawa, T. Sato, A. Yoshizawa, T. Inoue, W. Mori, *J. Catal.* **2005**, *230*, 226. c) C.-D. Wu, A. Hu, L. Zhang, W. Lin, *J. Am. Chem. Soc.* **2005**, *127*, 8940. d) O. Ohmori, M. Fujita, *Chem. Commun.* **2004**, 1586. e) J. A. Real, E. Andres, M. C. Munoz, M. Julve, T. Granier, A. Bousseksou, F. Varret, *Science* **1995**, *268*, 265.

9 a) M. Fujita, Y. J. Kwon, S. Washiza, K. Ogura, *J. Am. Chem. Soc.* **1994**, *116*, 1151. b) M. Munakata, L. P. Wu, T. Kuroda-Sowa, *Bull. Chem. Soc. Jpn.* **1997**, *70*, 1727. c) O. M. Yaghi, C. E. Davis, G. Li, H. Li, *J. Am. Chem. Soc.* **1997**, *119*, 2861. d) O. M. Yaghi, H. Li, C. Davis, D. Richardson, T. L. Groy, *Acc. Chem. Res.* **1998**, *31*, 474. e) S. C. Zimmerman, *Science* **1997**, *276*, 543.

10 B. C. H. Steele, A. Heinzel, *Nature* **2001**, *414*, 345.

11 a) J. A. Ritter, A. D. Ebner, J. Wang, R. Zidan, *Mater. Today* **2003**, *6*, 18. b) A. Züttel, *Mater. Today* **2003**, *6*, 24. c) J. M. Ogden, *Annu. Rev. Energy Env.* **1999**, *24*, 227.

12 a) Hydrogen, Fuel Cells, & Infrastructure Technologies Program: Multiyear Research, Development, and Demonstration Plan, U.S. Department of Energy, February, **2005**, Chap. 3, http://www.eere.energy.gov/hydrogenandfuelcells/mypp/. b) Basic Research Needs for the Hydrogen Economy in Report of the Basic Energy Sciences Workshop on Hydrogen Production, Storage, and Use, U.S. Department of Energy, May 13–15, **2005**, http://www.sc.doe.gov/bes/.

13 a) N. L. Rosi, J. Eckert, M. Eddaoudi, D. T. Vodak, J. Kim, M. O'Keeffe, O. M. Yaghi, *Science* **2003**, *300*, 1127. b) J. L. C. Rowsell, A. R. Millward, K. S. Park, O. M. Yaghi, *J. Am. Chem. Soc.* **2004**, *126*, 5666. c) J. L. C. Rowsell, O. M. Yaghi, *J. Am. Chem. Soc.* **2006**, *128*, 1304. d) A. G. Wong-Foy, A. J. Matzger, O. M. Yaghi, *J. Am. Chem. Soc.* **2006**, *128*, 3494. e) B. Panella, M. Hirscher, H. Pütter, U. Müller, *Adv. Funct. Mater.* **2006**, *16*,

520. f) H. Chun, D. N. Dybtsev, H. Kim, K. Kim, *Chem.—Eur. J.* **2005**, *11*, 3521. g) J. Jia, X. Lin, C. Wilson, A. J. Blake, N. R. Champness, P. Hubberstey, G. Walker, E. J. Cussen, M. Schröder, *Chem. Commun.* **2007**, 840. h) S. S. Kaye, J. R. Long, *J. Am. Chem. Soc.* **2005**, *127*, 6506. i) G. Férey, M. Latroche, C. Serre, F. Millange, T. Loiseau, A. Percheron-Guégan, *Chem. Commun.* **2003**, 2976. j) B. Xiao, P. S. Wheatley, X. Zhao, A. J. Fletcher, S. Fox, A. G. Rossi, I. L. Megson, S. Bordiga, L. Regli, K. M. Thomas, R. E. Morris, *J. Am. Chem. Soc.* **2007**, *129*, 1203.

14 W. Mori, F. Inoue, K. Yoshida, H. Nakayama, S. Takamizawa, M. Kishita, *Chem. Lett.* **1997**, 1219.

15 S. Takamizawa, W. Mori, M. Furihata, S. Takeda, K. Yamaguchi, *Inorg. Chim. Acta* **1998**, *283*, 268.

16 a) S. Takamizawa, K. Yamaguchi, W. Mori, *Inorg. Chem. Commun.* **1998**, *1*, 177. b) S. Takamizawa, T. Ohmura, K. Yamaguchi, W. Mori, *Mol. Cryst. Liq. Cryst.* **2000**, *342*, 199.

17 a) T. Ohmura, W. Mori, M. Hasegawa, T. Takei, A. Yoshizawa, *Chem. Lett.* **2003**, *32*, 34. b) T. Ohmura, W. Mori, M. Hasegawa, T. Takei, T. Ikeda, E. Hasegawa, *Bull. Chem. Soc. Jpn.* **2003**, *76*, 1387.

18 S. J. Gregg, K. S. W. Sing, *Adsorption, Surface Area and Porosity*, 2nd ed., Academic Press, London, U.K., **1982**.

19 T. Takei, T. Ii, J. Kawashima, T. Ohmura, M. Ichikawa, M. Hosoe, Y. Shinya, I. Kanoya, W. Mori, *Chem. Lett.* **2007**, *36*, 1136.

20 a) T. K. Maji, K. Uemura, H.-C. Chang, R. Matsuda, S. Kitagawa, *Angew. Chem.* **2004**, *116*, 3331. b) R. Wang, M. Hong, D. Yuan, Y. Sun, L. Xu, J. Luo, R. Cao, A. S. C. Chan, *Eur. J. Inorg. Chem.* **2004**, 37.

21 a) R. Kitaura, F. Iwahori, R. Matsuda, S. Kitagawa, Y. Kubota, M. Takata, T. C. Kobayashi, *Inorg. Chem.* **2004**, *43*, 6522. b) L. Pan, H. Li, S. P. Kelly, X. Huang, D. H. Olson, J. Li, *Chem. Commun.* **2003**, 854.

22 G. Horváth, K. Kawazoe, *J. Chem. Eng. Jpn.* **1983**, *16*, 470.

23 a) X. Zhao, B. Xiao, A. J. Fletcher, K. M. Thomas, D. Bradshaw, M. J. Rosseinsky, *Science* **2004**, *306*, 1012. b) B. Panella, M. Hirscher, *Adv. Mater.* **2005**, *17*, 538.

24 D. W. Breck, *Zeolite Molecular Sieves*, John Wiley & Sons, New York, **1974**.

25 H. Li, M. Eddaoudi, M. O'Keeffe, O. M. Yaghi, *Nature* **1999**, *402*, 276.

26 a) M. Rzepka, P. Lamp, M. A. de la Casa-Lillo, *J. Phys. Chem. B* **1998**, *102*, 10894. b) A. W. Adamson, *Physical Chemistry of Surfaces*, John Wiley & Sons, New York, **1990**.

27 G. J. Dash, *Films on Solid Surfaces*, Academic Press, London, **1975**.